

Lentiviral Delivery of a Vesicular Glutamate Transporter I (VGLUT1)-Targeting Short Hairpin RNA Vector Into the Mouse Hippocampus Impairs Cognition

Madeleine V King^{*,1,5}, Nisha Kurian^{1,6}, Si Qin^{2,3,7}, Nektaria Papadopoulou^{1,8}, Ben HC Westerink^{2,3}, Thomas I Cremers^{2,3,7}, Mark P Epping-Jordan⁴, Emmanuel Le Poul⁴, David E Ray^{1,10}, Kevin CF Fone^{1,5}, David A Kendall^{1,5}, Charles A Marsden^{1,5} and Tyson V Sharp^{1,9}

¹School of Biomedical Sciences, University of Nottingham Medical School, Queen's Medical Centre, Nottingham, UK; ²Department of Biomonitoring and Sensing, Groningen Research Institute of Pharmacy (GRIP), University of Groningen, Groningen, The Netherlands;

³Brains On-Line BV, Groningen, The Netherlands; ⁴Addex Pharmaceuticals SA, Chemin des Aulx, Geneva, Switzerland

Glutamate is the principle excitatory neurotransmitter in the mammalian brain, and dysregulation of glutamatergic neurotransmission is implicated in the pathophysiology of several psychiatric and neurological diseases. This study utilized novel lentiviral short hairpin RNA (shRNA) vectors to target expression of the vesicular glutamate transporter I (VGLUT1) following injection into the dorsal hippocampus of adult mice, as partial reductions in VGLUT1 expression should attenuate glutamatergic signaling and similar reductions have been reported in schizophrenia. The VGLUT1-targeting vector attenuated tonic glutamate release in the dorsal hippocampus without affecting GABA, and selectively impaired novel object discrimination (NOD) and retention (but not acquisition) in the Morris water maze, without influencing contextual fear-motivated learning or causing any adverse locomotor or central immune effects. This pattern of cognitive impairment is consistent with the accumulating evidence for functional differentiation along the dorsoventral axis of the hippocampus, and supports the involvement of dorsal hippocampal glutamatergic neurotransmission in both spatial and nonspatial memory. Future use of this nonpharmacological VGLUT1 knockdown mouse model could improve our understanding of glutamatergic neurobiology and aid assessment of novel therapies for cognitive deficits such as those seen in schizophrenia.

Neuropsychopharmacology (2014) **39**, 464–476; doi:10.1038/npp.2013.220; published online 25 September 2013

Keywords: VGLUT1; shRNA; hippocampus; glutamate; learning; memory

INTRODUCTION

Glutamate is the principal excitatory neurotransmitter in the mammalian brain where it contributes to learning, memory, and neuronal plasticity. Glutamate is transported into synaptic vesicles by three vesicular glutamate trans-

porters (VGLUTs 1–3), acts upon 11 receptors, and is cleared from the synaptic cleft by 5 excitatory amino acid transporters. Glutamatergic neurotransmission is further complicated by extrasynaptic release and the finding that altered extracellular glutamate can affect vesicular levels of its active metabolite, GABA (Shigeri *et al*, 2004).

Dysregulation of glutamatergic neurotransmission is implicated in the pathophysiology of several psychiatric and neurological diseases. For example, glutamate-induced excitotoxicity accompanies stroke or prolonged seizures, contributes to neurodegeneration (Danysz *et al*, 1995), and is implicated in angiogenesis (Mathew *et al*, 2008). In contrast, glutamatergic hypofunction may contribute to cognitive impairment commonly seen in schizophrenia and depression (Gaspar *et al*, 2009; Sharpley, 2009) that is resistant to drug treatment and a major factor preventing patient recovery. However, it is unclear how glutamate dysregulation arises and which synaptic components are involved. Pharmacological research is currently limited by a paucity of selective tools to subtly manipulate synaptic glutamate. There are no brain-penetrant agents that selectively target glutamate transporters, and pharmacological

*Correspondence: Dr MV King, School of Life Sciences, University of Nottingham, Medical School, Queen's Medical Centre, Nottingham NG7 2UH, UK, Tel: +44 (0)115 82 30402, Fax: +44 (0)115 82 30142, E-mail: madeleine.king@nottingham.ac.uk

⁵Current address: School of Life Sciences, University of Nottingham Medical School, Queen's Medical Centre, Nottingham, UK.

⁶Current address: R&I Bioscience, AstraZeneca, Pepparedsleden 1, Mölndal, SE-431 83, Sweden.

⁷Current address: Brains On-Line US LLC, 7000 Shoreline Court, South San Francisco, CA 94080, USA.

⁸Current address: Precos Ltd, Building 14, Hillcrest, Dodgeford Lane, Belton, Loughborough, UK.

⁹Current address: Barts Cancer Institute, Queen Mary University of London, John Vane Science Centre, Charterhouse Square, London, UK.

¹⁰Died on 14 November 2010.

Received 28 May 2013; revised 7 August 2013; accepted 8 August 2013; accepted article preview online 28 August 2013

blockade of single receptors is likely to have limited translational validity when modeling hypoglutamatergic states. Constitutive knockout of glutamate transporters causes major alterations in synaptic glutamate and can produce severe phenotypic alterations potentially confounded by developmental adaptations. Improved animal models of partial glutamate dysfunction are therefore required to explore the neurochemical basis of psychiatric disorders and to evaluate compounds that modulate glutamatergic neurotransmission.

This study utilized lentiviral short hairpin RNA (shRNA) vectors exploiting an evolutionarily conserved posttranscriptional gene-silencing mechanism (Thakker *et al*, 2006) to target dorsal hippocampal VGLUT1 expression and examine resultant cognitive dysfunction in adult mice. Lentiviral particles infect dividing and nondividing cells, including neurons (Naldini *et al*, 1996; Blömer *et al*, 1997), without inducing any major accompanying immune response. Virions remain localized to the injection site where their genetic material integrates into the host genome, resulting in prolonged intracellular shRNA generation (Kim *et al*, 2012) that enables partial but sustained brain region-specific protein knockdown in adult animals following a single intracerebral injection (Nielsen *et al*, 2009).

Although a single functional VGLUT appears sufficient to fill one synaptic vesicle with normal levels of glutamate, reduced transporter expression decreases the frequency of spontaneous quantal release at the *Drosophila* neuromuscular junction (Daniels *et al*, 2006) and reduces quantal size in rodent cortical and hippocampal cultures (Wojcik *et al*, 2004). Decreased transporter expression would therefore be expected to reduce glutamate signaling. Interestingly, the human VGLUT1 gene maps to chromosome 19q13, a possible susceptibility locus for schizophrenia (Hamshere *et al*, 2005; Francks *et al*, 2010). Furthermore, both VGLUT1 polymorphisms (Shen *et al*, 2009) and decreased hippocampal VGLUT1 expression have been reported in schizophrenia, particularly in older patients (Eastwood and Harrison, 2005; Sawada *et al*, 2005; Piyabhan and Reynolds, 2006), where they may contribute to cognitive dysfunction. To our knowledge, this study is the first to target regional VGLUT1 expression *in vivo* using lentiviral shRNA vectors, and focused on the dorsal hippocampus (where this transporter is most abundant in the adult; Shigeri *et al*, 2004) because of the pivotal role of hippocampal glutamate in cognitive processing (Izquierdo and Medina, 1997). The experiments reported herein were designed first to select a suitable vector for *in vivo* studies, based on the ability to knockdown VGLUT1 in a mouse neuroblastoma cell line. Having found no overt phenotypic abnormalities or any inflammatory response following localized intrahippocampal administration of this vector, subsequent behavioral studies evaluated its impact upon cognitive performance in tasks with translational relevance to cognitive domains deficient in schizophrenia. Finally, VGLUT1 expression was quantified and glutamatergic signaling examined (by microdialysis and microsensing) at timepoints corresponding to the key cognitive alterations. The timing of behavioral and neurochemical evaluations was similar to previous studies employing lentiviral shRNA delivery (Bahi and Dreyer, 2012a) and commenced 7 days

after intrahippocampal administration, as stable shRNA expression (Kim *et al*, 2012) and target mRNA (Bahi and Dreyer, 2012b) and protein (Nielsen *et al*, 2009) knockdown have been reported at this timepoint and importantly appear to be sustained beyond the 30-day duration of the current study.

MATERIALS AND METHODS

Lentiviral shRNA Vectors

Lentiviral pLKO.1-puro vectors containing a nontargeting control shRNA insert (with the sense strand indicated in bold; 5'-CCGGCAACAAGATGAAGAGCACCAACTCGAGTTGGTGCTCTTCATCTTGTGTTT-3') or one of five mouse VGLUT1 targeting inserts were obtained from MISSION TRC shRNA library (Sigma). VGLUT1 targeting sequences were as follows: VGLUT1 shRNA 1: 5'-CCGGTGAACCCTGT-TACGAAGTTTACTCGAGTAACTTCGTAACAGGGTTCATTTT-3'; VGLUT1 shRNA 2: 5'-CCGGGAACCCTGTTACGAAGTTTAACTCGAGTAACTTCGTAACAGGGTTCCTTTT-3'; VGLUT1 shRNA 3: 5'-CCGGGCCATCATCGTTGCGAAGTTTCTCGAGAAAGTTCGCAACGATGATGGCTTTTTG-3'; VGLUT1 shRNA 4: 5'-CCGGCGCCTACTTTGAAGAAGTGTCTCGAGAACACTTCTTCAAAGTAGGCGTTTTT-3'; and VGLUT1 shRNA 5: 5'-CCGGCGCCTAACCAATTCTACATTCTCGAGAAATGTAGAATTGGTTAGGCGTTTTT-3'. Lentiviral virions were produced by co-transfection of HEK293T cells with 5 µg pLKO.1-puro vector and 5 µg packaging and envelope vectors (Godfrey *et al*, 2005) using GeneJuice (Merck Biosciences). Media were harvested 48–72 h after transfection and centrifuged at 1500 g for 5 min. Supernatant was filtered (0.45 µm low protein binding filter; Sartorius Stedim Biotech) and used immediately for transduction of Neuro2A cells, or concentrated for *in vivo* administration by centrifugation at 20 000 g (4 h at 4 °C) and overnight resuspension in 1.5 ml phosphate-buffered saline (PBS; 4 °C). Aliquots were stored at –80 °C until determination of viral titer (QuickTiter Lentivirus Quantification kit; Cell Biolabs, according to the manufacturer's instructions) or *in vivo* administration, with a single freeze–thaw cycle in each case.

Transduction of Neuro2A Cells

Viral particles were transduced into 50–60% confluent Neuro2A cells by overnight incubation in equal volumes of growth media and nonconcentrated viral supernatant supplemented with protamine sulphate (10 µg/ml; Sigma). The following day, cells were superinfected using the same protocol. Stably transduced cells were selected with 5 µg/ml puromycin (Invivogen) for 14 days, starting 48 h after transduction.

qRT-PCR

Total RNA was isolated from Neuro2A cells or mouse dorsal hippocampi using TRiPure Isolation reagent (Roche Applied Sciences) according to the manufacturer's instructions, treated with recombinant RNase-free DNase-1 (Roche Applied Sciences) to remove any genomic DNA contamination, and purified using a standard phenol–chloroform

extraction. Then, 1 μ g total RNA was reverse-transcribed into cDNA using the Transcriptor first-strand cDNA synthesis kit (Roche Applied Sciences), and quantitative PCR designed using the Universal ProbeLibrary Assay Design Centre. Primers and probes were as follows: VGLUT1 forward: 5'-GTGCAATGACCAAGCACAAG-3' reverse: 5'-AGATGACACCGCCGTAGTG-3'; 36B4 acidic ribosomal protein reference gene forward: 5'-GATGCCAGGGAAGACAG-3' reverse: 5'-ACAATGAAGCATTTTGGATAATCA-3' (MWG-Biotech AG). Assays were performed using FastStart Universal Probe master (Rox; Roche Applied Sciences) according to the manufacturer's instructions in an ABI Prism 7000HT sequence detection system (Applied Biosystems). Data were normalized to expression of 36B4.

Western Blots

Neuro2A cells or mouse dorsal hippocampi were homogenized in lysis buffer (20 mM Tris, 1 mM EGTA, 320 mM sucrose, 0.1% Triton X-100, 1 mM NaF, 10 mM β -glycerophosphate) containing a protease inhibitor cocktail (Roche Applied Sciences). Proteins (15 μ g per lane) were electrophoresed on 10% SDS-PAGE gels (200 V, 40 min) and then transferred onto nitrocellulose membranes, blocked with 5% nonfat milk in Tris-buffered saline-Tween 20 (150 mM NaCl, 50 mM Tris-HCl, 0.05% Tween-20; pH7.4), and incubated overnight (4 °C) with a monoclonal VGLUT1 (1:500; Chemicon) or β -actin (1:20 000; Sigma) primary antibody. Visualization was achieved using a horseradish peroxidase-conjugated secondary antibody (1:2000, Dako) by autoradiography and quantified using a Bio-Rad GS 710 imaging densitometer. Data were normalized to expression of β -actin.

Animals

A total of 70 adult male C57Bl6/J mice were obtained from Charles River, UK ($n = 38$ for behavioral testing followed by qRT-PCR and western blotting or immunohistochemistry) or Harlan, The Netherlands ($n = 32$ for microdialysis and microsensing). They were housed individually on a 12 h light/dark cycle (lights on at 0700 h) with constant environmental conditions (temperature 21 ± 2 °C, relative humidity $55 \pm 10\%$) and *ad libitum* access to food and water. Procedures were carried out in accordance with the UK Animals (Scientific Procedures) Act (1986) with approval of the University of Nottingham Local Ethical Review Committee (behavioral studies), or in accordance with the NIH guidelines for the care and use of laboratory animals with approval of the University of Groningen Animal Care Committee (microdialysis and microsensing).

Stereotaxic Vector Injections Into Mouse Hippocampus

Mice were anesthetized with isoflurane in oxygen and nitrous oxide and then placed in a stereotaxic frame. The skull surface was exposed and holes drilled at the injection sites. Mice received bilateral injections of nontarget control shRNA or VGLUT1 shRNA 5' encoding lentiviral vectors (2 μ l per side; 9.68×10^7 viral particles/ μ l, a similar titer to previous studies; Ortiz *et al*, 2010) into the dorsal

hippocampus (anterioposterior -2.0 , mediolateral ± 1.5 , dorsoventral -2.5 mm from Bregma) using a 33-gauge microinjector connected to a Hamilton syringe. Injections occurred over 2 min and the injector remained in place for a further 2 min. Injection sites were sealed with bone wax, and wounds sutured and then treated with Xylocaine local anesthetic, Fuciderm topical antibiotic, and Nobecutane plastic dressing. Mice received subcutaneous Rimadyl analgesia (10 μ l/kg) and saline (0.25 ml) to prevent post-operative pain and dehydration. Wet mash was provided for 4 days after surgery in the home cage.

Behavioral Test Battery

Mice ($n = 16$) underwent a 1-h locomotor activity test (as described below) on day 1 to allow balanced allocation of nontarget control or VGLUT1 shRNA 5' vector injections on days 2–3. Postsurgery behavioral assessments were selected to initially evaluate gross behavioral responses to the VGLUT1-targeting shRNA lentiviral vector with the subsequent emphasis on cognitive function (using methods adapted from Scullion *et al*, 2011), and were ordered from the least to most aversive.

Neurobehavioral observations and rotarod testing. Testing commenced with a neurobehavioral observation battery, consisting of home cage and open-field observation and neuromuscular and sensory motor tests (Moscardo *et al*, 2007) on day 9 (6–7 days after surgery). This was followed by rotarod testing on day 10 (7–8 days after surgery; five trials at 30 min intervals, assessing latency to fall from a rod revolving at 16 r.p.m., for a maximum of 180 s).

Locomotor activity. Postsurgery locomotor activity was assessed over a 60-min period on day 11 (8–9 days after surgery) in one of eight identical novel arenas ($30 \times 17 \times 25.5$ cm) using an EthoVision video tracking system (Noldus Information Technology).

Novel object discrimination (NOD). Testing was performed on day 12 (9–10 days after surgery) in the same arenas used for locomotor activity assessment. Mice received a 10-min familiarization trial with two identical painted wooden objects, a 1-h interval in the home cage, and a 10-min choice trial with one novel and one familiar object (previously cleaned with 20% (v/v) ethanol to remove olfactory cues). Exploration of each object (sniffing, licking, chewing, or having moving vibrissae while directing the nose ≤ 1 cm toward the object) was timed from videotape by an observer unaware of treatment.

Morris water maze. Water maze training began on day 15 (12–13 days after surgery) with a 60-s swim in a pool of opaque water (23 °C), followed by practice of climbing onto a submerged 10 cm platform in the center of the maze. For the next 3 days, mice received two sessions (2–3 h apart) of three trials with a constant platform location (in the center of a randomly assigned quadrant) and variable starting point. Latency to reach the platform (maximum 60 s) and swim speed were recorded using EthoVision. On day 19, 24 h after the final acquisition trial, the platform was

removed for a 60-s probe trial (16–17 days after surgery). Time spent in a 30-cm annulus around the learned platform position and equivalent control annuli in the three other pool quadrants were recorded.

Prepulse inhibition of acoustic startle (PPI). PPI was assessed on day 22 (19–20 days after surgery) using a SR-Lab Startle Response System (San Diego Instruments). After 5 min of acclimatization (65 dB white noise), mice received six startle-alone trials (120 dB), a pseudorandom mix of startle preceded by 0, 68, 72, or 80 dB prepulse (12 of each), and then the final six startle-alone trials, separated by a variable unpredictable interval (10–20 s). Individual whole-body startle responses were recorded for a 100-ms period from the onset of the startle pulse and used to calculate a total cumulative area under the curve.

Contextual fear conditioning. Mice received a 10-min acquisition trial (day 25; 22–23 days after surgery) with one 0.4 mA foot shock every min, and then were returned to the same box 24 h later for a 3-min retention trial with no foot shocks. Distance moved during each trial was automatically determined, and freezing behavior was manually recorded using EthoVision by an observer unaware of treatment.

Tissue collection. Mice were killed 27–30 days after lentiviral vector administration by sequential intracardiac perfusion of 0.154 M saline and then 4% paraformaldehyde under terminal anesthesia to provide brains for VGLUT1 immunohistochemistry and confirmation of the injection site. Separate mice ($n=6$) were killed immediately after NOD testing by the same method to provide brains for Cd11b immunohistochemistry, or by concussion and immediate cervical dislocation ($n=16$) to provide dorsal hippocampi for qRT-PCR and western blot analysis of VGLUT1 mRNA and protein expression at the same postsurgery timepoint where key cognitive deficits were identified.

Microdialysis

At 6 days after lentiviral vector administration, mice ($n=16$) were anesthetized with isoflurane while concentric microdialysis probes with a 2-mm active polyacrylonitrile membrane (Brainlink) were implanted at the injection coordinates in the right hippocampus and secured to the skull with dental acrylic. The following day, Ringer's solution (147 mM NaCl, 3 mM KCl, 1.2 mM CaCl₂; pH 6.4) was perfused through the probe (1.5 μ l/min) using a CMA/102 microdialysis pump (CMA Microdialysis AB). After 1.5 h of stabilization, baseline samples were collected into 7.5 μ l 0.02 M formic acid (FA) at 15 min intervals for 2 h. The glutamate reuptake inhibitor DL-threo- β -benzyloxyaspartate (TBOA; Tocris), which blocks excitatory amino acid transporters 1–3 and increases extracellular glutamate, was then introduced into the perfusate (300 μ M) to facilitate detection of tonic glutamate release and sampling continued for 2 h. Samples were stored at -80°C until analysis with high-performance liquid chromatography with tandem mass spectrometry (LC-MS/MS). Probe position within the dorsal hippocampus was verified histologically in all

animals. Samples (10 μ l) were mixed with internal standard (1.2 μ M [D₅]-glutamate; Cambridge Isotope Laboratories, and 30 nM [D₆]-GABA; Isotec) and automatically derivatized by addition of 40 μ l SymDAQ (symmetrical dialdehyde quaternary ions) reagent in the autosampler (SIL-10AD vp, Shimadzu). After a 2-min reaction time, 40 μ l was injected into the LC system for chromatographic separation on a reversed-phase Hypersil Gold column (50 \times 2.1 mm; 1.9 μ m particle size) held at 40 $^{\circ}\text{C}$. Components were separated using a linear gradient of acetonitrile (ACN) and FA in ultrapure water (flow rate 0.3 ml/min) according to the following scheme: 0 min = 3% ACN, 0.1% FA; 3.5 min = 35% ACN, 0.1% FA; 4.5 min = 90% ACN, 0.1% FA; 5.5 min = 3% ACN, 0.1% FA. After 2 min of eliminating waste, the flow was switched to MS for detection of glutamate and GABA. MS analyses were performed with an API 4000MS/MS system consisting of an API 3000MS/MS detector and a Turbo Ion Spray interface (Applied Biosystems) in positive ionization mode (ion spray voltage 4 kV, probe temperature 200 $^{\circ}\text{C}$) with multiple reaction monitoring. Data were calibrated and quantified using Analyst software (Applied Biosystems; version 1.4.2).

Microsensors

Ceramic-based platinum microelectrode arrays with four 15 \times 333 μ m recording sites (S2 type) were obtained from Quanteon LLC and prepared for glutamate detection by immobilization of glutamate oxidase onto the two sites closest to the tip (Burmeister *et al*, 2002). The remaining two sites were coated with enzyme-free protein matrix to serve as background electrodes for self-referencing. After curing the enzyme layer at room temperature (>48 h), an outer poly-*m*-phenylenediamine membrane was applied by cyclic voltammetry (3 cycles/min from +250 to +750 mV vs Ag/AgCl for a total of 22 min in 5 mM poly-*m*-phenylenediamine). To permit local administration of test compounds by Hamilton syringe, a glass capillary micropipette was mounted on a custom-built sensor holder and the tip (25–30 μ m i.d.) positioned ~ 200 μ m from the midpoint of glutamate and background electrodes, at an angle of 15–20 $^{\circ}$. Before implantation, microelectrode arrays were calibrated *in vitro* at +700 mV vs an Ag/AgCl reference electrode, in the presence of 250 μ M ascorbic acid, 20–60 μ M glutamate, 2 μ M dopamine, and 8.8 μ M H₂O₂ using a computer-controlled FAST-16mkII recording system (Quanteon LLC; Burmeister *et al*, 2002; Day *et al*, 2006), and then stored in PBS until use and recalibrated again immediately after experiment to correct for biofouling. At 7 days after lentiviral vector administration, mice ($n=16$) were anesthetized with isoflurane and the sensor and micropipette implanted at the injection coordinates in the right hippocampus, and an Ag/AgCl reference electrode placed under the skull. A continuous potential of +700 mV vs this reference was applied, and the FAST-16mkII system was used to record glutamate signals every second after subtraction of background current. Once a stable baseline was observed (~ 1 h after implantation), 400 nl 1 mM TBOA was applied via the micropipette and recording continued for 1 h. Sensor positioning within the dorsal hippocampus was verified histologically in all animals.

Immunohistochemistry

Paraffin-embedded coronal brain sections obtained immediately after NOD testing on day 10 after lentiviral vector administration (Cd11b; 10 μ m) or on days 27–30 after administration (VGLUT1; 5 μ m) were mounted on 3-aminopropyltriethoxysilane (APES)-coated slides. They were dewaxed and rehydrated before antigen retrieval (10 mM sodium citrate pH 6; 20 min at 95 °C followed by 20 min gentle agitation without further heating) and endogenous peroxidase activity was eliminated with 3% hydrogen peroxide in methanol (10 min).

Cd11b. Cd11b is a marker of microglial activation. Sections were blocked in PBS containing 2% rabbit serum (30 min) and incubated (90 min) with monoclonal rat anti-mouse Cd11b primary antibody (1:50; AbD serotec) or blocking solution alone for negative control. They were washed three times with PBS and then incubated (60 min) with polyclonal rabbit anti-rat secondary antibody (1:100; Dako), all at room temperature. Visualization was achieved with 3,3'-diaminobenzidine (DAB), followed by counterstaining with hematoxylin and eosin.

VGLUT1. Sections were blocked in PBS containing 1.5% goat serum (60 min; VECTASTAIN rabbit ABC Kit; Vector Laboratories) and then incubated (60 min at room temperature and then 4 °C overnight) with polyclonal rabbit anti-rat VGLUT1 primary antibody alone (1:1000; Synaptic Systems) or preadsorbed with VGLUT1 control peptide (Synaptic Systems) as the negative control. Sections were washed, incubated for 60 min with biotinylated goat anti-rabbit secondary antibody (1:200; VECTASTAIN rabbit ABC Kit), washed, and then incubated for 30 min with ABC reagent (VECTASTAIN rabbit ABC Kit). Sections received three final PBS washes before visualization with DAB and counterstaining with hematoxylin. Sections were dehydrated and coverslipped with DPX mounting medium and then digital photographs obtained using a Leica DM4000B microscope, Q Imaging micropublisher 3.3 RTV camera, and Openlab software (PerkinElmer). Immunoreactivity was quantified with Volocity software (PerkinElmer) within an area 20 μ m wide \times 25 μ m high (chosen to exclude any cell nuclei that would otherwise interfere with quantification) spanning a region 30–50 μ m from the center of the injection tract in the stratum lacunosum-moleculare of CA1. Tissue from nontarget control and VGLUT1-targeting shRNA-treated groups was processed in parallel to prevent any nonspecific difference in intensity level. As a further precaution, data from each animal were normalized to the signal intensity in an equivalent size area of stratum lacunosum-moleculare spanning 100–120 μ m from the injection tract in the same slice.

Statistical Analysis

Comparisons between two groups used two-tailed Student's unpaired *t*-tests for parametric data or, in the case of basal extracellular GABA levels, Mann–Whitney *U*-tests, based on the outcome of Shapiro–Wilk normality tests. Comparisons between more groups at a single timepoint used one-way ANOVA, and those involving multiple trials or timepoints

utilized two-way repeated measures ANOVA with Bonferroni's multiple comparison or Tukey's *post hoc* tests. Analyses were performed using Sigmapstat or GraphPad Prism software (version 5.02) and $P < 0.05$ was considered significant.

RESULTS

Validation of shRNA-Induced VGLUT1 Knockdown *In Vitro*

Before using lentiviral shRNA vectors to target VGLUT1 expression in the mouse hippocampus *in vivo*, knockdown efficiency was confirmed *in vitro* after stable transduction into a mouse neuroblastoma cell line. qRT-PCR revealed a significant decrease in VGLUT1 mRNA expression in Neuro2A cells following each of the five VGLUT1-targeting sequences (one-way ANOVA: $F_{(5,12)} = 16.370$, $P < 0.0001$; Figure 1a), with the most profound decrease (87%) being achieved with VGLUT1 shRNA 5 ($P < 0.001$ vs non-target control; Bonferroni's multiple comparison *post hoc*). Although western blots performed at the same timepoint suggested similar protein knockdown with all VGLUT1-targeting shRNA vectors (Figure 1b), this was less extensive than for mRNA ($\sim 26\%$; Figure 1c), and the effect of shRNA sequence failed to reach statistical significance (one-way ANOVA: $F_{(5,12)} = 0.400$, $P > 0.05$). This most likely reflects a low rate of VGLUT1 protein turnover in cultured cells in the absence of stimulated glutamate release, and VGLUT1-targeting shRNA 5 was selected for progression to *in vivo* studies based on the highly significant knockdown of VGLUT1 mRNA achieved with this sequence *in vitro* (Figure 1a).

Intrahippocampal Administration of Lentiviral shRNA Vectors Did Not Affect Motor Coordination or Exploratory Activity

Before intrahippocampal administration of lentiviral shRNA vectors, mice assigned to nontarget control and VGLUT1-targeting shRNA groups were of equal body weight and exhibited equivalent locomotor activity during a 1-h period in a novel arena. All mice gained weight following surgery, with no between-group differences at any point during the 26-day test battery (day: $F_{(20,280)} = 82.68$, $P < 0.0001$; shRNA sequence: $F_{(1,280)} = 0.375$, $P > 0.05$; interaction: $F_{(20,280)} = 1.683$, $P < 0.05$, but Bonferroni's multiple comparison *post-hoc* tests $P > 0.05$).

Neither control nor VGLUT1-targeting shRNA-treated mice demonstrated any adverse behavioral effects during the neurobehavioral assessment. Core body temperature remained normal and was not affected by shRNA sequence (37.9 ± 0.1 °C in controls and 37.9 ± 0.2 °C following VGLUT1-targeting shRNA; $P > 0.05$). The only significant between-group difference during this neurobehavioral assessment was a decrease in supported rearing by VGLUT1-targeting shRNA-treated mice during a 3-min period in an open field (7.0 ± 1.5 rears compared with 13.3 ± 1.3 in controls; $P < 0.01$). When balance and motor coordination were further assessed 24 h later using a rotarod, the latency to fall from the apparatus decreased across trials ($F_{(4,56)} = 9.613$, $P < 0.0001$) but was unaffected by treatment

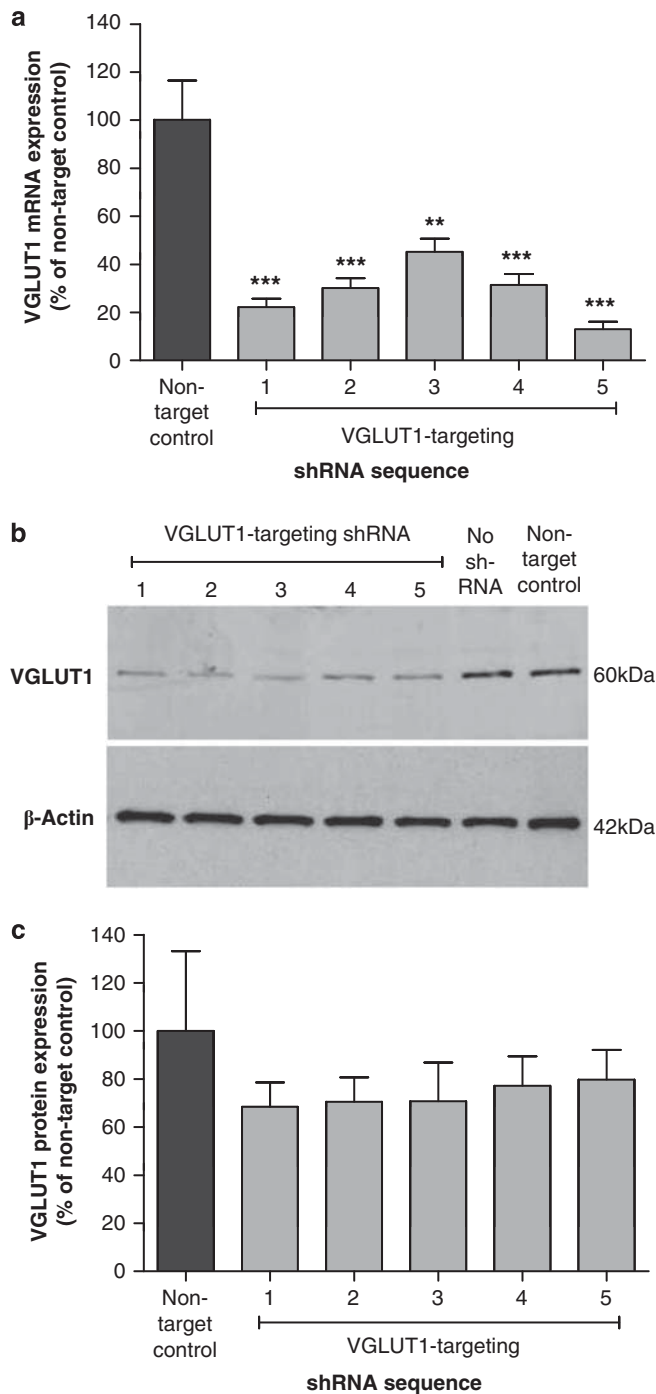


Figure 1 Impact of lentiviral shRNA vectors on VGLUT1 expression in Neuro2A cells. (a) Mean (\pm SEM) levels of VGLUT1 mRNA in stably transduced cells were normalized to expression of the acidic ribosomal protein 36B4, and expressed as a percentage of those following control nontargeting shRNA. All of the VGLUT1-targeting shRNAs produced significant mRNA knockdown (** $P < 0.01$; *** $P < 0.001$ vs nontarget control; Bonferroni's multiple comparison *post hoc* following one-way ANOVA. (b) Representative image of western blot showing VGLUT1 and β -actin protein expression in stably transduced cells (for clarity, gels have been cropped to exclude regions over six band widths from VGLUT1 and β -actin bands). (c) Mean (\pm SEM) levels of VGLUT1 protein normalized to expression of β -actin and presented as a percentage of those following control nontargeting shRNA. Statistics were performed on raw data and not the percentage change, and $n = 3$ in each case.

($F_{(1,56)} = 0.015$, $P > 0.05$), and there was no significant treatment \times trial interaction ($F_{(4,56)} = 0.784$, $P > 0.05$).

When locomotor activity was assessed in a novel arena, there was no significant effect of treatment on total distance moved throughout the 1 h session (control, 115.8 ± 7.7 m and VGLUT1-targeting shRNA, 109.5 ± 3.5 m; $P > 0.05$) or during any particular successive 5 min time epoch (time: $F_{(11,154)} = 1.587$, $P > 0.05$; shRNA sequence: $F_{(1,154)} = 0.570$, $P > 0.05$; interaction: $F_{(11,154)} = 0.388$, $P > 0.05$). Furthermore, analysis of simultaneous rearing behavior revealed no significant differences at these timepoints or during the first 3 min (15.5 ± 1.6 supported rears in controls and 13.0 ± 1.2 following VGLUT1-targeting shRNA; $P > 0.05$). Taken together, these findings demonstrate that neither of the shRNA vectors induced any overt phenotypic abnormalities incompatible with further cognitive testing, and immunohistochemical examination of brains from shRNA-treated mice (10 days after surgery) revealed no inflammatory response to lentiviral delivery at the timepoint corresponding to key cognitive alterations. Thus, staining for Cd11b, a marker of microglial activation, was confined to the needle tract, with no obvious lesion at the tip and no evidence of any cellular reaction $> 30 \mu\text{m}$ from the center of the tract in either treatment group (data not shown).

Intrahippocampal Administration of VGLUT1-Targeting shRNA Causes Specific Memory Impairments

To examine the effect of VGLUT1-targeting shRNA 5 on learning and memory, mice underwent a range of tasks with translational relevance to three distinct cognitive domains affected in schizophrenia (Young *et al*, 2009; Orosz *et al*, 2008). First, nonspatial visual recognition memory was examined using a hippocampal-dependent NOD task (Hammond *et al*, 2004; Broadbent *et al*, 2004) based on rodents innate preference for novelty, rather than food reward or negative reinforcement, which therefore involves similar motivational conditions to those under which human memory is normally assessed. Control and VGLUT1-targeting shRNA-treated mice achieved comparable levels of object exploration during the acquisition phase of this task (91.1 ± 6.6 and 74.9 ± 5.3 s, respectively; $P > 0.05$) and showed no preference for either of the identical objects ($F_{(1,14)} = 2.281$, $P > 0.05$; shRNA sequence: $F_{(1,14)} = 3.682$, $P > 0.05$; interaction: $F_{(1,14)} = 0.069$, $P > 0.05$; Figure 2a). In the choice trial 1 h later, the two groups of mice exhibited significantly different patterns of object exploration (object: $F_{(1,14)} = 62.490$, $P < 0.0001$; shRNA sequence: $F_{(1,14)} = 0.003$, $P > 0.05$; interaction: $F_{(1,14)} = 24.660$, $P < 0.001$). Control mice showed a clear exploratory preference for the novel object ($P < 0.001$; Figure 2b), indicating intact visual recognition memory. In contrast, mice that had received intrahippocampal injections of the VGLUT1-targeting lentiviral shRNA vector 9–10 days earlier were unable to discriminate the novel from the familiar object ($P > 0.05$; Figure 2b), and exhibited a significantly lower choice trial discrimination ratio (time at novel object/total choice trial object exploration) than controls (0.52 ± 0.01 compared with 0.59 ± 0.01 in controls; $P < 0.001$). Importantly, this alteration in cognitive performance resulted in a redistribution of exploration during the choice trial without any significant alteration in the total

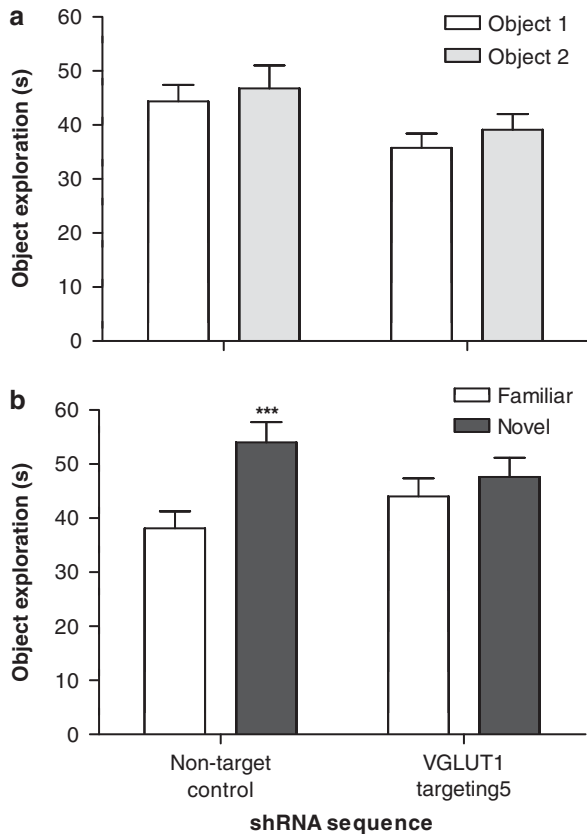


Figure 2 Intrahippocampal delivery of a VGLUT1-targeting lentiviral shRNA vector selectively impairs memory retention in a mouse novel object discrimination task (performed 9–10 days after injection). (a) Mean (\pm SEM) exploration of two identical objects during the familiarization trial was unaffected by treatment. (b) Mean (\pm SEM) exploration of novel and familiar objects during the choice trial. Discrimination occurred in control mice, but was impaired by VGLUT1-targeting shRNA (***) ($P < 0.001$ vs the familiar object in the same treatment group; Bonferroni's multiple comparison *post hoc* following two-way repeated measures ANOVA); $n = 8$ in each case.

level of object-directed attention (control, 92.1 ± 6.8 s; VGLUT1, 91.6 ± 6.6 s; $P > 0.05$).

When spatial learning and memory were assessed in the same mice using a hippocampal-dependent (Broadbent *et al*, 2004; Cho *et al*, 1999) Morris water maze task, control and VGLUT1-targeting shRNA-treated mice demonstrated comparable acquisition of the submerged platform location such that both groups showed a progressive reduction in the latency to reach the platform across the acquisition phase, and both groups reached the same final level of performance irrespective of shRNA treatment (trial: $F_{(17,238)} = 2.571$, $P < 0.001$; shRNA sequence: $F_{(1,238)} = 0.019$, $P > 0.05$; interaction: $F_{(17,238)} = 1.027$, $P > 0.05$; Figure 3a). In marked contrast, at 24 h after the final acquisition trial, with the platform removed from the maze, the two groups of mice exhibited significantly different swim patterns (annulus location: $F_{(3,42)} = 8.451$, $P < 0.001$; shRNA sequence: $F_{(1,42)} = 0.902$, $P > 0.05$; interaction: $F_{(3,42)} = 2.964$, $P < 0.05$). Control mice spent significantly longer searching a 30-cm annulus around the learned platform position than comparable-sized annuli in opposite

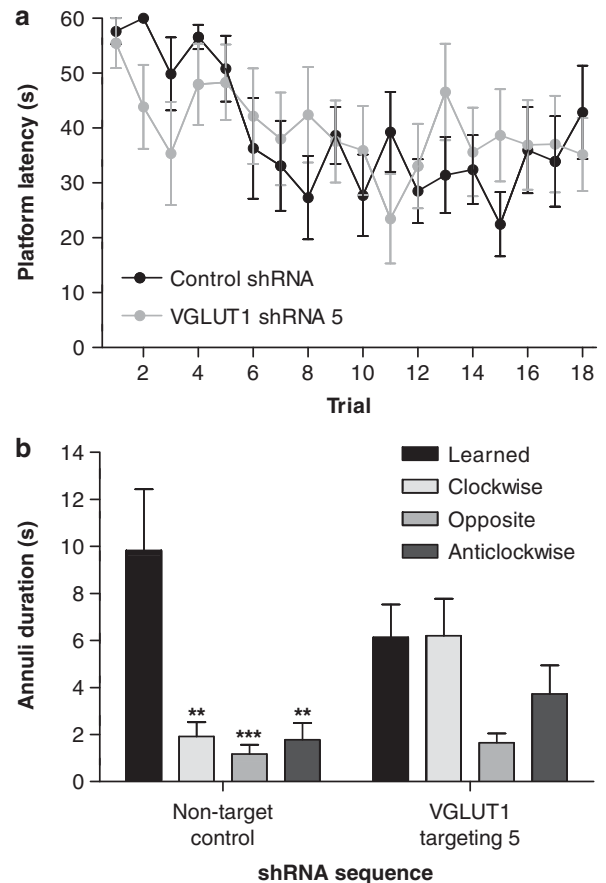


Figure 3 Intrahippocampal delivery of a VGLUT1-targeting lentiviral shRNA vector selectively impairs memory retention in a mouse water maze task (ending 16–17 days after injection) without affecting acquisition. (a) Mean (\pm SEM) latency to locate the submerged platform during acquisition training was unaffected by treatment. (b) Mean (\pm SEM) duration spent in a 30-cm annulus around the learned platform position and control 30-cm annuli in nonplatform quadrants of the maze (clockwise, opposite, and anticlockwise). Retention of the learned platform position occurred in control mice, but was impaired by VGLUT1-targeting shRNA (***) ($P < 0.001$ vs the learned annulus in the same treatment group; Bonferroni's multiple comparison *post hoc* following one-way ANOVA); $n = 8$ in each case.

($P < 0.001$) or adjacent ($P < 0.01$) quadrants of the maze (one-way ANOVA: $F_{(3,28)} = 9.716$, $P < 0.0001$), whereas mice that received the VGLUT1-targeting lentiviral shRNA vector 16–17 days earlier showed no such preference (one-way ANOVA: $F_{(3,28)} = 2.428$, $P > 0.05$; Figure 3b). Importantly, this difference in probe trial swim pattern occurred without any significant alteration in total distance traveled (control, 9.5 ± 1.0 m; VGLUT1, 9.8 ± 0.8 m; $P > 0.05$) or swim speed (control, 16.0 ± 1.7 cm/s; VGLUT1, 16.5 ± 1.3 cm/s; $P > 0.05$).

PPI is a well-recognized measure of sensorimotor gating and preattentive processing, which is deficient in patients with schizophrenia (Young *et al*, 2009) and known to be regulated by the hippocampus, prefrontal cortex, amygdala, striatum, nucleus accumbens, and thalamus (Koch, 1999; Swerdlow *et al*, 2001). In the current study, when PPI was examined 19–20 days after lentiviral vector administration, control and VGLUT1-targeting shRNA-treated mice both exhibited the normal attenuation of startle by increased prepulse amplitude ($F_{(3,52)} = 6.585$, $P < 0.001$) with no main

effect of shRNA sequence ($F_{(1,52)} = 0.313$, $P > 0.05$) or any shRNA \times prepulse interaction ($F_{(3,52)} = 0.221$, $P > 0.05$). There was no difference in basal reactivity (control, 159.1 ± 19.6 , VGLUT1, 156.0 ± 22.1 ; $P > 0.05$) or habituation to the startle pulse across the test session (control, $32.2 \pm 12.2\%$, VGLUT1, $32.5 \pm 10.2\%$; $P > 0.05$).

Cognitive testing concluded with assessment of associative learning and memory in a contextual fear conditioning task. Although not part of the MATRICS cognitive battery (Young *et al*, 2009), this task was included as it is dependent on the hippocampus (in addition to the amygdala, which mediates cued conditioning without any hippocampal involvement; Phillips and LeDoux, 1992) and there is strong evidence that associative learning and memory is impaired in patients with schizophrenia (Orosz *et al*, 2008). With the administration of consecutive foot shocks during the acquisition session, control and VGLUT1-targeting shRNA-treated mice exhibited comparable decreases in locomotor activity ($F_{(9,126)} = 80.65$, $P < 0.0001$) and increases in freezing duration ($F_{(9,126)} = 30.89$, $P < 0.0001$) with no effect of treatment (locomotor activity: $F_{(1,126)} = 0.385$, $P > 0.05$; freezing duration: $F_{(1,126)} = 1.946$, $P > 0.05$) or any treatment \times time interaction (locomotor activity: $F_{(9,126)} = 0.299$, $P > 0.05$; freezing duration: $F_{(9,126)} = 0.911$, $P > 0.05$), thereby confirming that the expected associative learning occurred with no confounding effects of shRNA sequence on anxiety or sensory perception. During the retention trial 24 h later, locomotor activity and freezing duration were again unaffected by treatment ($F_{(1,28)} = 0.718$, $P > 0.05$ and $F_{(1,28)} = 0.035$, $P > 0.05$, respectively) and there was no treatment \times time interaction (locomotor activity: $F_{(2,28)} = 0.536$, $P > 0.05$ and $F_{(1,28)} = 0.005$, $P > 0.05$, respectively), showing that the VGLUT1-targeting shRNA sequence had no effect on retention of contextual fear-motivated associative memory in the absence of further foot shocks.

Intrahippocampal Administration of VGLUT1-Targeting shRNA Selectively Attenuates Glutamatergic Neurotransmission

In order to quantify shRNA-induced VGLUT1 knockdown *in vivo*, dorsal hippocampi were collected from a separate group of mice on day 10 after injection for determination of target mRNA and protein levels at a timepoint corresponding to one of the key cognitive deficits (having also confirmed reproduction of the aforementioned NOD impairment in these mice). qRT-PCR and western blot analyses of these relatively large tissue samples (mean wet weight 5.99 ± 0.26 mg; 45% of total hippocampus) revealed only modest depletion of VGLUT1 mRNA (22%) and protein (17%) that failed to reach statistical significance (VGLUT1 mRNA expression normalized to that of 36B4 was 1.21 ± 0.15 in controls and 0.94 ± 0.13 following VGLUT1-targeting shRNA; $P > 0.05$, and VGLUT1 protein expression normalized to that of β -actin was 0.23 ± 0.04 in controls and 0.19 ± 0.04 following VGLUT1-targeting shRNA; $P > 0.05$). To provide an indication of whether shRNA-induced VGLUT1 knockdown occurred in a restricted area close to the intrahippocampal injection site, immunohistochemistry was performed using tissue obtained after completion of the full behavioral test battery (27–30 days after lentiviral vector administration). The observed pattern of VGLUT1 immu-

noreactivity in the dorsal hippocampus of control mice was consistent with previous reports (Bellocchio *et al*, 1998; Fremeau *et al*, 2001; Varoqui *et al*, 2002) demonstrating widespread expression, with the exception of granule and pyramidal cell layers, and particular enrichment in stratum oriens and radiatum of CA1 as well as the molecular and polymorphic layers of the dentate gyrus (Figure 4a, left). All VGLUT1 staining was abolished by preadsorption of the primary antibody with a VGLUT1 control peptide (data not shown). VGLUT1-targeting shRNA appeared to cause a focal decrease in VGLUT1 immunoreactivity that extended $\sim 100 \mu\text{m}$ from the center of the needle tract and was most evident in stratum lacunosum-moleculare of CA1 and the polymorphic layer of the dentate gyrus (Figure 4). Signal

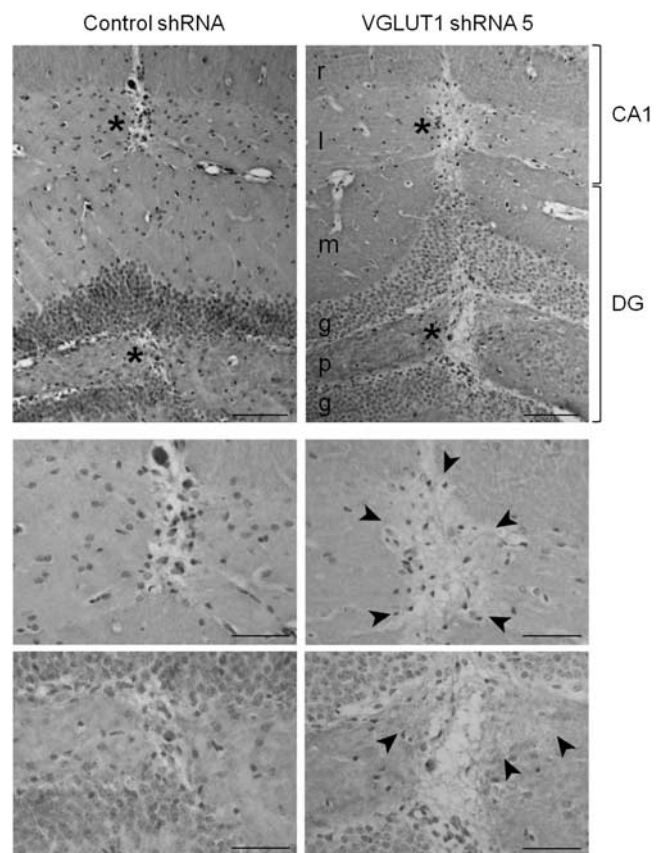


Figure 4 Intrahippocampal delivery of a VGLUT1-targeting lentiviral shRNA vector appears to reduce VGLUT1 expression in neurons adjacent to the injection tract. (a) Representative low-power images of immunohistochemical staining for VGLUT1 (DAB; brown) in the dorsal hippocampus 27 days after administration of control nontargeting shRNA (left) or VGLUT1-targeting shRNA (right). Nuclei are counterstained with hematoxylin (purple). Asterisks positioned to the left of the needle tract illustrate the location of the higher-power images of (b) the CA1 stratum lacunosum-moleculare and (c) the polymorphic cell layer of the dentate gyrus. Arrowheads indicate the apparent visual boundary of reduced VGLUT1 expression following administration of the VGLUT1-targeting shRNA vector. However, signal intensity in a $20 \times 25 \mu\text{m}$ area of stratum lacunosum-moleculare positioned $30 \mu\text{m}$ from the center of the injection tract (and normalized to an equivalent area $100 \mu\text{m}$ from the injection tract in the same slice) was significantly reduced by the VGLUT1-targeting vector (0.92 ± 0.01 compared with 1.0 ± 0.02 in controls; $P < 0.05$). Scale bar: (a) $100 \mu\text{m}$; (b, c) $50 \mu\text{m}$. DG, dentate gyrus; g, granule cell layer; l, stratum lacunosum-moleculare; m, molecular layer; p, polymorphic cell layer; r, stratum radiatum. A full color version of this figure is available at the *Neuropsychopharmacology*, journal online.

intensity in a $20 \times 25 \mu\text{m}$ area of stratum lacunosum-moleculare (spanning a region $30\text{--}50 \mu\text{m}$ from the center of the injection tract, normalized to intensity in an equivalent area $70 \mu\text{m}$ further away, and expressed as a ratio thereof) was significantly reduced by the VGLUT1-targeting vector (0.92 ± 0.01 compared with 1.00 ± 0.02 in controls; $P < 0.05$).

In order to determine if this small localized change in protein expression in the hippocampal tissue could be accompanied by a marked change in function *in vivo*, microdialysis and LC-MS/MS were used to assess glutamate and GABA efflux within the dorsal hippocampus of freely moving mice on day 7 after injection. There was no significant effect of VGLUT1-targeting shRNA on basal levels of extracellular glutamate (control, $0.395 \pm 0.179 \mu\text{M}$; VGLUT1, $0.499 \pm 0.257 \mu\text{M}$; $P > 0.05$), but the increase

in glutamate efflux observed on inclusion of the glutamate reuptake inhibitor TBOA in the perfusate (time: $F_{(15,209)} = 31.339$, $P < 0.001$) was significantly attenuated by VGLUT1-targeting shRNA (shRNA sequence: $F_{(1,209)} = 2.729$, $P > 0.05$; interaction: $F_{(15,209)} = 2.223$, $P < 0.01$; Figure 5a). It is noteworthy that this change occurred without any significant effect on either basal (control, $21.00 \pm 3.153 \text{ nM}$; VGLUT1, $17.710 \pm 2.741 \text{ nM}$; $P > 0.05$) or TBOA-evoked increases in extracellular GABA efflux (time: $F_{(15,210)} = 14.680$, $P < 0.0001$; shRNA sequence: $F_{(1,210)} = 0.547$, $P > 0.05$; interaction: $F_{(15,210)} = 0.678$, $P > 0.05$).

Although the majority of GABA efflux measured by microdialysis fulfills the criteria for exocytotic release, basal glutamate detected with this technique is not calcium dependent or sensitive to sodium channel blockade by tetrodotoxin (van der Zeyden *et al*, 2008), suggesting it is largely of extrasynaptic origin. In contrast, recently developed glutamate microsensors (enzyme-coated micro-electrode arrays coupled with electrochemical detection) provide greater spatial and temporal resolution than microdialysis, and evidence shows that part of the basal glutamate efflux detected by this method is tetrodotoxin sensitive (Day *et al*, 2006). This complimentary technique was therefore used to measure extracellular glutamate concentrations in the dorsal hippocampus of anesthetized mice on day 7 after injection. Despite the possibility that the two techniques may sample different glutamate pools, findings with microsensors matched those with microdialysis, there being no significant effect of VGLUT1-targeting shRNA on basal levels of extracellular glutamate (control, $9.75 \pm 2.409 \mu\text{M}$; VGLUT1, $10.00 \pm 1.932 \mu\text{M}$; $P > 0.05$) but a significantly attenuated area under the curve response to TBOA microinjection in VGLUT1-targeting shRNA-treated mice ($P < 0.05$; Figure 5b).

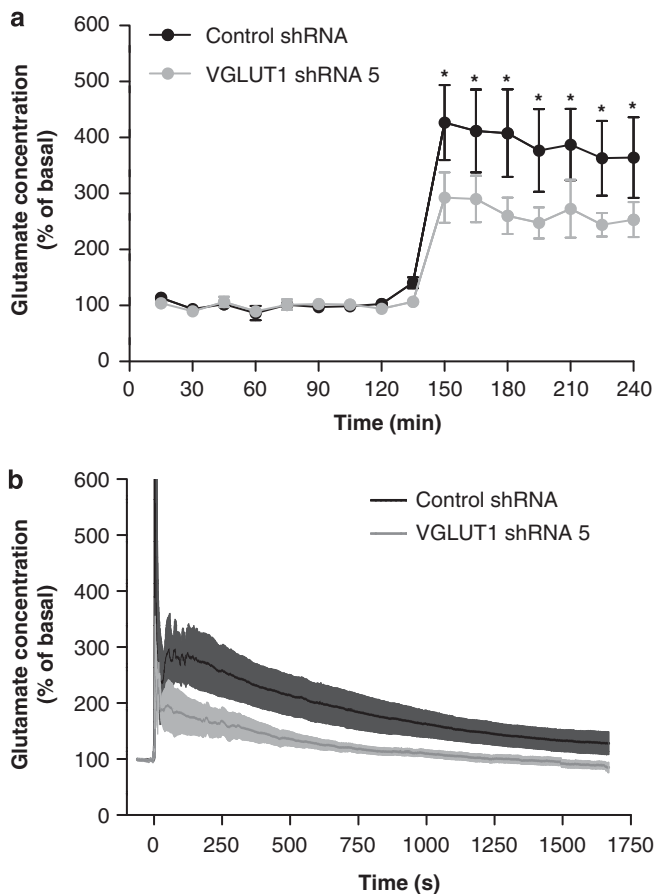


Figure 5 Intra-hippocampal delivery of a VGLUT1-targeting lentiviral shRNA vector attenuates TBOA-evoked increases in extracellular glutamate (assessed 7 days after injection). (a) Extracellular glutamate concentrations determined by microdialysis in freely moving animals, expressed as a percentage (mean \pm SEM) of average basal values in the 60 min immediately before TBOA infusion ($300 \mu\text{M}$). TBOA-evoked increases in extracellular glutamate were attenuated by VGLUT1-targeting shRNA ($*P < 0.05$ vs nontarget control; Tukey's *post hoc* following two-way repeated measures ANOVA). (b) Extracellular glutamate concentrations detected by glutamate microsensors in anesthetized mice, expressed as a percentage (mean \pm SEM) of average basal values in the 10 s immediately before local injection of TBOA (1 mM , 400 nl). Total area under the curve following TBOA administration was significantly reduced by VGLUT1-targeting shRNA ($P < 0.05$ vs nontarget control; two-tailed Student's *t*-test); $n = 8$ in each case.

DISCUSSION

A particular strength of RNA interference techniques is that they can be directed at protein targets for which selective pharmacological tools are unavailable and, as such, offer great promise for examining both the physiological and pathological roles of CNS proteins, and for generating novel animal models of neurological and psychiatric disorders (Thakker *et al*, 2006). This present study is the first to use RNA interference to target the expression of VGLUT1 in a specific brain region *in vivo* as a novel means of manipulating synaptic glutamate release. Hippocampal expression of VGLUT1 mRNA and protein is decreased in schizophrenia (Eastwood and Harrison, 2005; Sawada *et al*, 2005; Piyabhan and Reynolds, 2006) and, although striatal deficits have also been reported (Piyabhan and Reynolds, 2006; Nudmamud-Thanoi *et al*, 2007), cortical changes (which do occur in depression; Gilabert-Juan *et al*, 2012) are far less robust in schizophrenia (Corti *et al*, 2007; Oni-Orisan *et al*, 2008; Uezato *et al*, 2009; Eastwood and Harrison, 2010) and appear restricted to specific layers of the prefrontal cortex (Eastwood and Harrison, 2005; Bitanhirwe *et al*, 2009), whereas the amygdala remains unaffected (Varea *et al*, 2012). The principal finding of the current study is that administration of a VGLUT1-targeting lentiviral shRNA vector into the dorsal hippocampus of

adult mice caused a localized reduction in tonic glutamate release accompanied by selective memory impairments in both nonspatial NOD and spatial Morris water maze tasks. These deficits in visual learning and memory were achieved without the more global phenotypic changes associated with marked perturbation of glutamatergic neurotransmission by glutamate receptor antagonists.

Targeting whole-brain VGLUT1 expression using conventional gene knockout strategies results in a 35–41% decrease in transporter levels in heterozygous animals (Tordera *et al*, 2007; Garcia-Garcia *et al*, 2009). These mice exhibit anxiety and a ‘depressive-like’ phenotype accompanied by deficits in working, social, and visual recognition memory and impaired PPI, reversal learning, fear extinction, and hippocampal long-term potentiation (Tordera *et al*, 2007; Garcia-Garcia *et al*, 2009; Balschun *et al*, 2010; Elizalde *et al*, 2010; Inta *et al*, 2012; Callaerts-Vegh *et al*, 2013). The latter is consistent with the fact that VGLUT1 localizes to synapses with low release probability (that exhibit long-term potentiation), whereas VGLUT2 localizes to synapses with high release probability (that exhibit long-term depression; Varoqui *et al*, 2002). In the current study, localized targeting of VGLUT1 expression within the dorsal hippocampus induced deficits in visual recognition and spatial memory that were actually more marked than those observed in VGLUT1 heterozygotes. For example, Tordera *et al* (2007) reported impaired long-term memory in a 24-h intertrial interval version of the NOD task but normal performance of VGLUT1 heterozygotes with a 1-h intertrial interval as used in the present study, and Garcia-Garcia *et al* (2009) detected a NOD deficit with a 1-h intertrial interval only after previous exposure to chronic mild stress. Two independent groups also failed to observe any impairment of VGLUT1 heterozygous mice during acquisition or probe trials in a Morris water maze reference memory task similar (but not identical) to that used in the present study (Tordera *et al*, 2007; Balschun *et al*, 2010). The apparent spread of lentiviral particles following intrahippocampal injection is reported to be <0.5 mm using similar injection apparatus, rate, and volume of administration to the current study (Kanninen *et al*, 2009), and hence only ~17% of the dorsal hippocampal tissue used for quantification of VGLUT1 mRNA and protein levels is likely to have been exposed to the VGLUT1-targeting shRNA vector. Immunohistochemical analysis of VGLUT1 expression in coronal brain slices showed a localized selective reduction extending ~100 µm from the injection tract in VGLUT1-targeting shRNA-treated mice (but not controls) and being most evident in the stratum lacunosum-moleculare of CA1 and the polymorphic layer of the dentate gyrus. This is consistent with the proposal that the extent of VGLUT1 knockdown close to the injection site may be greater than the estimated 22 and 17% decreases in respective mRNA and protein levels measured in the entire dorsal hippocampus, and in a small subset of dorsal hippocampal neurons the reduction in VGLUT1 expression in this study could perhaps be greater than the 35–41% knockdown previously reported in heterozygous VGLUT1 knockout mice. This may explain the more marked impairment in NOD and water maze performance seen herein. VGLUT1 is expressed in a distinct laminar pattern throughout the dorsal hippocampus, with particular enrichment in the

polymorphic and molecular cell layers. Localization to strata oriens and radiatum of CA1 suggests expression in terminals of the Schaffer collateral system, presence in stratum lucidum of CA3 represents expression in mossy fiber terminals from dentate granule cells, and stronger labeling in outer regions of the molecular layer of the dentate gyrus indicates preferential localization to perforant path inputs from the entorhinal cortex (Bellocchio *et al*, 1998; Fremeau *et al*, 2001; Varoqui *et al*, 2002). Despite low VGLUT2 expression in the pyramidal layer of CA2 and the granular layer of the dentate gyrus (Fremeau *et al*, 2001), there is no evidence for coexpression of both transporters within individual nerve terminals (Herzog *et al*, 2001), and a recent detailed study found no evidence for VGLUT1 expression in hippocampal astrocytes (Li *et al*, 2013). Use of some hippocampal tissue for qRT-PCR and western blots prevented verification of the injection site in every animal, but all sites that were examined were in either the dentate gyrus or CA1 regions. Although the change in VGLUT1 expression in the current study was sufficient to cause a 35% decrease in functional measures of tonic glutamate release close to the injection site, it is not known how this compares with glutamate efflux in VGLUT1 heterozygotes as there are no published reports of microdialysis or microsensor measurements in these mice. However, another potentially important factor is the presence of alterations in GABAergic neurotransmission in VGLUT1 heterozygotes. Despite normal tissue glutamate levels, these animals exhibit a 35–46% reduction in tissue GABA levels within the hippocampus and frontal cortex (Tordera *et al*, 2007; Garcia-Garcia *et al*, 2009) that contrasts with the current lack of impact of VGLUT1-targeting shRNA on basal extracellular levels of GABA or in tonic GABA release in the presence of TBOA.

The observed pattern of cognitive impairments in the present study may reflect the differing motivational status during the NOD and water maze tasks compared with contextual fear conditioning, but it also appears to be consistent with the accumulating evidence for functional differentiation along the dorsoventral (septotemporal) axis of the hippocampus (Moser and Moser, 1998; Bast and Feldon, 2003). For example, permanent lesions of the rat dorsal hippocampus consistently impair spatial memory in the Morris water maze (with probe tests being more sensitive than final escape latencies; Moser *et al*, 1993), but can spare contextual fear conditioning in both rats (Maren *et al*, 1997) and mice (Frankland *et al*, 1998). In contrast, ventral lesions can spare spatial memory (Moser *et al*, 1993) while impairing contextual fear conditioning (Fanselow and Dong, 2010) and attenuating PPI (Bast and Feldon, 2003). Potential contributions of the ventral hippocampus to NOD have yet to be investigated, but this task certainly involves dorsal regions of the mouse hippocampus as temporary inactivation by localized administration of lignocaine into the CA1 region impairs performance, provided that a sufficient long intertrial interval is used (Hammond *et al*, 2004). This apparent functional differentiation is consistent with changes in afferent and efferent connectivity along the dorsoventral axis of the hippocampus. The dorsal pole receives predominantly sensory information from cortical association areas and the olfactory bulb via the lateral entorhinal

cortex, and sends projections to regions involved in visuospatial learning and memory, navigation, and exploratory activity, including the retrosplenial and anterior cingulate cortices, lateral mammillary nuclei, anterior thalamus, and indirectly, ventral tegmental area and substantia nigra (Fanselow and Dong, 2010). In contrast, the ventral pole receives inputs from and sends projections to regions involved in motivation, emotion, affective state, and sensorimotor gating, including the amygdala, hypothalamus, prefrontal cortex, medial septum, and nucleus accumbens (Moser and Moser, 1998; Koch, 1999; Bast and Feldon, 2003; Fanselow and Dong, 2010). Taken together, these observations appear to explain the selective impact of the VGLUT1-targeting shRNA vector on NOD and Morris water maze performance following its administration into the dorsal hippocampus. Indeed, the current findings further support the involvement of dorsal hippocampal glutamatergic neurotransmission in both spatial and non-spatial visual learning and memory. Future research beyond the scope of the current study could attempt to use glutamate microsensors in freely moving animals to quantify glutamate release during cognitive tasks, where VGLUT1 shRNA-induced deficits in glutamatergic neurotransmission may be even more apparent. Continued use of this translationally relevant animal model, created without any pharmacological intervention, in conjunction with microdialysis, microsensors, and pharmacological MRI could improve our understanding of the neurobiology of schizophrenia and depression, and aid assessment of novel therapies for the drug-resistant cognitive symptoms.

FUNDING AND DISCLOSURE

The authors declare no conflict of interest.

ACKNOWLEDGEMENTS

BHCW, TIC, MPE-J, ELP, CAM and TVS conceived the studies, and MPE-J & ELP were leaders of the AGLAEA consortium. MVK designed and carried out all of the behavioral experiments and immunohistochemistry, and wrote the manuscript (with contributions to relevant sections from NK, SQ and TVS). NK generated the lentiviral virions (with assistance from NP) and carried out the Neuro2A cell experiments. SQ designed and carried out the microdialysis and microsensor experiments. BHCW and TIC supervised the microdialysis and microsensor experiments, DER supervised the Cd11b immunohistochemistry, KCFF, DAK, and CAM supervised the behavioral experiments and VGLUT1 immunohistochemistry, and TVS supervised lentiviral virion generation and the Neuro2A cell experiments. All authors discussed the results and commented on the manuscript. We acknowledge Denise Christie, Maxine Fowler, Liaque Latif, Stacey Knapp, Maureen Mee, Marie Smith, Clare Spicer, and Ian Ward (University of Nottingham) and Corry Hofland, Ar Jansen, Karola Jansen, and Jelle Kleijn (University of Groningen/Brains On-Line) for providing technical assistance, and Raffaella Catena (ALMA Consulting Group, Lyon, France) for her contribution to the AGLAEA Consortium. This research was funded by the European Commission through

the Sixth Framework Programme for Research and Development (LSHM-CT-2006-037554).

REFERENCES

- Bahi A, Dreyer JL (2012a). Hippocampus-specific deletion of tissue plasminogen activator 'tPA' in adult mice impairs depression- and anxiety-like behaviors. *Eur Neuropsychopharmacol* **22**: 672–682.
- Bahi A, Dreyer JL (2012b). Involvement of nucleus accumbens dopamine D1 receptors in ethanol drinking, ethanol-induced conditioned place preference, and ethanol-induced psychomotor sensitization in mice. *Psychopharmacology (Berl)* **222**: 141–153.
- Balschun D, Moechars D, Callaerts-Vegh Z, Vermaercke B, Van Acker N, Andries L et al (2010). Vesicular glutamate transporter VGLUT1 has a role in hippocampal long-term potentiation and spatial reversal learning. *Cereb Cortex* **20**: 684–693.
- Bast T, Feldon J (2003). Hippocampal modulation of sensorimotor processes. *Prog Neurobiol* **70**: 319–345.
- Bellocchio EE, Hu H, Pohorille A, Chan J, Pickel VM, Edwards RH (1998). The localization of the brain-specific inorganic phosphate transporter suggests a specific presynaptic role in glutamatergic transmission. *J Neurosci* **18**: 8648–8659.
- Bitanirwe BK, Lim MP, Kelley JF, Kaneko T, Woo TU (2009). Glutamatergic deficits and parvalbumin-containing inhibitory neurons in the prefrontal cortex in schizophrenia. *BMC Psychiatry* **9**: 71.
- Blömer U, Naldini L, Kafri T, Trono D, Verma IM, Gage FH (1997). Highly efficient and sustained gene transfer in adult neurons with a lentivirus vector. *J Virol* **71**: 6641–6649.
- Burmeister JJ, Pomerleau F, Palmer M, Day BK, Huettl P, Gerhardt GA (2002). Improved ceramic-based multisite microelectrode for rapid measurements of L-glutamate in the CNS. *J Neurosci Methods* **119**: 163–171.
- Broadbent NJ, Squire LR, Clark RE (2004). Spatial memory, recognition memory, and the hippocampus. *Proc Natl Acad Sci USA* **101**: 14515–14520.
- Callaerts-Vegh Z, Moechars D, Van Acker N, Daneels G, Goris I, Leo S et al (2013). Haploinsufficiency of VGluT1 but not VGluT2 impairs extinction of spatial preference and response suppression. *Behav Brain Res* **245**: 13–21.
- Cho YH, Friedman E, Silva AJ (1999). Ibotenate lesions of the hippocampus impair spatial learning but not contextual fear conditioning in mice. *Behav Brain Res* **98**: 77–87.
- Corti C, Crepaldi L, Mion S, Roth AL, Xuereb JH, Ferraguti F (2007). Altered dimerization of metabotropic glutamate receptor 3 in schizophrenia. *Biol Psychiatry* **62**: 747–755.
- Daniels RW, Collins CA, Chen K, Gelfand MV, Featherstone DE, DiAntonio A (2006). A single vesicular glutamate transporter is sufficient to fill a synaptic vesicle. *Neuron* **49**: 11–16.
- Danysz W, Parsons CG, Bresink I, Quack G (1995). Glutamate in CNS disorders. *Drug News Perspect* **8**: 261–277.
- Day BK, Pomerleau F, Burmeister JJ, Huettl P, Gerhardt GA (2006). Microelectrode array studies of basal and potassium-evoked release of L-glutamate in the anesthetized rat brain. *J Neurochem* **96**: 1626–1635.
- Eastwood SL, Harrison PJ (2005). Decreased expression of vesicular glutamate transporter 1 and complexin II mRNAs in schizophrenia: further evidence for a synaptic pathology affecting glutamate neurons. *Schizophr Res* **73**: 159–172.
- Eastwood SL, Harrison PJ (2010). Markers of glutamate synaptic transmission and plasticity are increased in the anterior cingulate cortex in bipolar disorder. *Biol Psychiatry* **67**: 1010–1016.
- Elizalde N, Pastor PM, Garcia-García AL, Serres F, Venzala E, Huarte J et al (2010). Regulation of markers of synaptic function

- in mouse models of depression: chronic mild stress and decreased expression of VGLUT1. *J Neurochem* **114**: 1302–1314.
- Fanselow MS, Dong HW (2010). Are the dorsal and ventral hippocampus functionally distinct structures? *Neuron* **65**: 7–19.
- Francks C, Tozzi F, Farmer A, Vincent JB, Rujescu D, St, Clair D *et al* (2010). Population-based linkage analysis of schizophrenia and bipolar case-control cohorts identifies a potential susceptibility locus on 19q13. *Mol Psychiatry* **15**: 319–325.
- Frankland PW, Cestari V, Filipkowski RK, McDonald RJ, Silva AJ (1998). The dorsal hippocampus is essential for context discrimination but not for contextual conditioning. *Behav Neurosci* **112**: 863–874.
- Fremeau RT Jr, Troyer MD, Pahner I, Nygaard GO, Tran CH, Reimer RJ *et al* (2001). The expression of vesicular glutamate transporters defines two classes of excitatory synapse. *Neuron* **31**: 247–260.
- García-García AL, Elizalde N, Matrov D, Harro J, Wojcik SM, Venzala E *et al* (2009). Increased vulnerability to depressive-like behavior of mice with decreased expression of VGLUT1. *Biol Psychiatry* **66**: 275–282.
- Gaspar PA, Bustamante ML, Silva H, Aboitiz F (2009). Molecular mechanisms underlying glutamatergic dysfunction in schizophrenia: therapeutic implications. *J Neurochem* **111**: 891–900.
- Gilbert-Juan J, Varea E, Guirado R, Blasco-Ibáñez JM, Crespo C, Nacher J (2012). Alterations in the expression of PSA-NCAM and synaptic proteins in the dorsolateral prefrontal cortex of psychiatric disorder patients. *Neurosci Lett* **530**: 97–102.
- Godfrey A, Anderson J, Papanastasiou A, Takeuchi Y, Boshoff C (2005). Inhibiting primary effusion lymphoma by lentiviral vectors encoding short hairpin RNA. *Blood* **105**: 2510–2518.
- Hammond RS, Tull LE, Stackman RW (2004). On the delay-dependent involvement of the hippocampus in object recognition memory. *Neurobiol Learn Mem* **82**: 26–34.
- Hamshere ML, Bennett P, Williams N, Segurado R, Cardno A, Norton N *et al* (2005). Genome wide linkage scan in schizoaffective disorder: significant evidence for linkage at 1q42 close to DISC1, and suggestive evidence at 22q11 and 19p13. *Arch Gen Psychiatry* **62**: 1081–1088.
- Herzog E, Bellenchi GC, Gras C, Bernard V, Ravassard P, Bedet C *et al* (2001). The existence of a second vesicular glutamate transporter specifies subpopulations of glutamatergic neurons. *J Neurosci* **21**: RC181.
- Inta D, Vogt MA, Perreau-Lenz S, Schneider M, Pfeiffer N, Wojcik SM *et al* (2012). Sensorimotor gating, working and social memory deficits in mice with reduced expression of the vesicular glutamate transporter VGLUT1. *Behav Brain Res* **228**: 328–332.
- Izquierdo I, Medina JH (1997). Memory formation: the sequence of biochemical events in the hippocampus and its connection to activity in other brain structures. *Neurobiol Learn Mem* **68**: 285–316.
- Kanninen K, Heikkinen R, Malm T, Rolova T, Kuhmonen S, Leinonen H *et al* (2009). Intrahippocampal injection of a lentiviral vector expressing Nrf2 improves spatial learning in a mouse model of Alzheimer's disease. *Proc Natl Acad Sci USA* **106**: 16505–16510.
- Kim CS, Chang PY, Johnston D (2012). Enhancement of dorsal hippocampal activity by knockdown of HCN1 channels leads to anxiolytic- and antidepressant-like behaviors. *Neuron* **75**: 503–516.
- Koch M (1999). The neurobiology of startle. *Prog Neurobiol* **59**: 107–128.
- Li D, Héroult K, Silm K, Evrard A, Wojcik S, Oheim M *et al* (2013). Lack of evidence for vesicular glutamate transporter expression in mouse astrocytes. *J Neurosci* **33**: 4434–4455.
- Maren S, Aharonov G, Fanselow MS (1997). Neurotoxic lesions of the dorsal hippocampus and Pavlovian fear conditioning in rats. *Behav Brain Res* **88**: 261–274.
- Mathew SJ, Price RB, Charney DS (2008). Recent advances in the neurobiology of anxiety disorders: implications for novel therapeutics. *Am J Med Genet C Semin Med Genet* **148C**: 89–98.
- Moscardo E, Maurin A, Dorigatti R, Champeroux P, Richard S (2007). An optimised methodology for the neurobehavioural assessment in rodents. *J Pharmacol Toxicol Methods* **56**: 239–255.
- Moser E, Moser MB, Andersen P (1993). Spatial learning impairment parallels the magnitude of dorsal hippocampal lesions, but is hardly present following ventral lesions. *J Neurosci* **13**: 3916–3925.
- Moser MB, Moser EI (1998). Functional differentiation in the hippocampus. *Hippocampus* **8**: 608–619.
- Naldini L, Blömer U, Gage FH, Trono D, Verma IM (1996). Efficient transfer, integration, and sustained long-term expression of the transgene in adult rat brains injected with a lentiviral vector. *Proc Natl Acad Sci USA* **93**: 11382–11388.
- Nielsen TT, Iv Marion, Hasholt L, Lundberg C (2009). Neuron-specific RNA interference using lentiviral vectors. *J Gene Med* **11**: 559–569.
- Nudmamud-Thanoi S, Piyabhan P, Harte MK, Cahir M, Reynolds GP (2007). Deficits of neuronal glutamatergic markers in the caudate nucleus in schizophrenia. *J Neural Transm Suppl* **72**: 281–285.
- Oni-Orisan A, Kristiansen LV, Haroutunian V, Meador-Woodruff JH, McCullumsmith RE (2008). Altered vesicular glutamate transporter expression in the anterior cingulate cortex in schizophrenia. *Biol Psychiatry* **63**: 766–775.
- Orosz AT, Feldon J, Gal G, Simon AE, Cattapan-Ludewig K (2008). Deficient associative learning in drug-naive first-episode schizophrenia: results obtained using a new visual within-subjects learned irrelevance paradigm. *Behav Brain Res* **193**: 101–107.
- Ortiz O, Delgado-García JM, Espadas I, Bahí A, Trullas R, Dreyer JL *et al* (2010). Associative learning and CA3-CA1 synaptic plasticity are impaired in D1R null, *Drd1a* $-/-$ mice and in hippocampal siRNA silenced *Drd1a* mice. *J Neurosci* **30**: 12288–12300.
- Phillips RG, LeDoux JE (1992). Differential contribution of amygdala and hippocampus to cued and contextual fear conditioning. *Behav Neurosci* **106**: 274–285.
- Piyabhan P, Reynolds GP (2006). Striatal and hippocampal vesicular glutamate transporter-1 deficit in schizophrenia and affective disorders. *J Psychopharmacol* **20S**: A18.
- Sawada K, Barr AM, Nakamura M, Arima K, Young CE, Dwork AJ *et al* (2005). Hippocampal complexin proteins and cognitive dysfunction in schizophrenia. *Arch Gen Psychiatry* **62**: 263–272.
- Scullion GA, Kendall DA, Marsden CA, Sunter D, Pardon MC (2011). Chronic treatment with the α 2-adrenoceptor antagonist fluparoxan prevents age-related deficits in spatial working memory in APP \times PS1 transgenic mice without altering β -amyloid plaque load or astrogliosis. *Neuropharmacology* **60**: 223–234.
- Sharpley CF (2009). Malfunction in GABA and glutamate as pathways to depression: a review of the evidence. *Clin Med Ther* **1**: 1511–1519.
- Shen YC, Liao DL, Chen JY, Wang YC, Lai IC, Liou YJ *et al* (2009). Resequencing and association study of vesicular glutamate transporter 1 gene (VGLUT1) with schizophrenia. *Schizophr Res* **115**: 254–260.
- Shigeri Y, Seal RP, Shimamoto K (2004). Molecular pharmacology of glutamate transporters, EAATs and VGLUTs. *Brain Res Brain Res Rev* **45**: 250–265.
- Swerdlow NR, Geyer MA, Braff DL (2001). Neural circuit regulation of prepulse inhibition of startle in the rat: current knowledge and future challenges. *Psychopharmacology (Berl)* **156**: 194–215.
- Thakker DR, Hoyer D, Cryan JF (2006). Interfering with the brain: use of RNA interference for understanding the pathophysiology of psychiatric and neurological disorders. *Pharmacol Ther* **109**: 413–438.
- Tordera RM, Totterdell S, Wojcik SM, Brose N, Elizalde N, Lasheras B *et al* (2007). Enhanced anxiety, depressive-like behaviour and impaired recognition memory in mice with reduced expression of the vesicular glutamate transporter 1 (VGLUT1). *Eur J Neurosci* **25**: 281–290.

- Uezato A, Meador-Woodruff JH, McCullumsmith RE (2009). Vesicular glutamate transporter mRNA expression in the medial temporal lobe in major depressive disorder, bipolar disorder, and schizophrenia. *Bipolar Disord* **11**: 711–725.
- van der Zeyden M, Oldenziel WH, Rea K, Cremers TI, Westerink BH (2008). Microdialysis of GABA and glutamate: analysis, interpretation and comparison with microsensors. *Pharmacol Biochem Behav* **90**: 135–147.
- Varea E, Guirado R, Gilabert-Juan J, Martí U, Castillo-Gomez E, Blasco-Ibáñez JM *et al* (2012). Expression of PSA-NCAM and synaptic proteins in the amygdala of psychiatric disorder patients. *J Psychiatr Res* **46**: 189–197.
- Varoqui H, Schäfer MK, Zhu H, Weihe E, Erickson JD (2002). Identification of the differentiation-associated Na⁺/P₁ transporter as a novel vesicular glutamate transporter expressed in a distinct set of glutamatergic synapses. *J Neurosci* **22**: 142–155.
- Wojcik SM, Rhee JS, Herzog E, Sigler A, Jahn R, Takamori S *et al* (2004). An essential role for vesicular glutamate transporter 1 (VGLUT1) in postnatal development and control of quantal size. *Proc Natl Acad Sci USA* **101**: 7158–7163.
- Young JW, Powell S, Risbrough V, Marston HM, Geyer MA (2009). Using the MATRICS to guide development of a preclinical cognitive test battery for research in schizophrenia. *Pharmacol Ther* **122**: 150–202.